Proceedings of the IASTED International Conference
Signal Processing, Pattern Recognition and Applications (SPPRA 2012)
June 18 - 20, 2012 Crete, Greece

ISTHMUS–BASED ORDER–INDEPENDENT SEQUENTIAL THINNING

Péter Kardos
Department of Image Processing and Computer Graphics
University of Szeged
Szeged, Hungary
email: pkardos@inf.u-szeged.hu

Kálmán Palágyi
Department of Image Processing and Computer Graphics
University of Szeged
Szeged, Hungary
email: palagyi@inf.u-szeged.hu

ABSTRACT
Thinning as a layer-by-layer reduction is a frequently used technique for skeletonization. Sequential thinning algorithms usually suffer from the drawback of being order-dependent, i.e., their results depend on the visiting order of object points. Earlier order-independent sequential methods are based on the conventional thinning schemes that preserve endpoints to provide relevant geometric information of objects. These algorithms can generate centerlines in 2D and medial surfaces in 3D. This paper presents an alternative strategy for order-independent thinning which follows an approach, proposed by Bertrand and Couprie, which accumulates so-called isthmus points. The main advantage of this order-independent strategy over the earlier ones is that it makes also possible to produce centerlines of 3D objects.

KEY WORDS
image representation, skeleton, sequential thinning, order–independency, digital topology

1 Introduction

Skeleton is a fundamental shape descriptor used in many fields of image processing and pattern recognition [15]. Thinning is an iterative object reduction of binary objects in a topology preserving way [16]. Typical skeleton-like shape features are the *centerline* of 2D and 3D objects and the *medial surface* of 3D objects. Topological thinning algorithms are based on the concept of *simple point*s. An object point is said to be a simple point, if its deletion (i.e., changing it to background point) preserves the topology [9]. In 2D, it means that no object is split nor completely deleted, no cavity is merged with the background nor another cavity, and no cavity is created [7]. There is an additional concept called hole in 3D binary pictures. Topology preservation implies that eliminating or creating any hole is not allowed [8].

In order to produce skeleton-like shape features, both sequential and parallel alternatives of thinning algorithms were proposed [11]. Algorithm 1 sketches the general two-phase scheme for sequential thinning. The basic criterion for a “deletable” point is usually that it must be a simple point but not a so-called *endpoint*, since preserving endpoints provides relevant geometrical information relative to the shape of the objects. Another thinning strategy is proposed by Bertand and Couprie that is based on the accumulation of some non-simple points called *isthmus*es [2]. Characterizations of these isthmuses were firstly defined by Bertrand and Aktouf [1].

Algorithm 1:

```
repeat
    // Phase 1: contour tracking
    mark all simple points
    // Phase 2: reduction
    foreach marked point p do
        if p is "deletable" in the actual image then
            delete p
until no points are deleted
```

The most important advantage of sequential thinning methods over parallel ones is that topology preservation can be easily ensured by removing only one simple point at a time [11]. However in sequential thinning, the resulting skeleton usually depends on the visiting order of object points.

In order to overcome this problem, order–independent sequential thinning methods were proposed. The solutions for the 2D case originating from Ranwez and Soille [12] and by Iwanowski and Soille [4] do not retain endpoints which are important in the view of shape-preservation. This results in the disadvantage that, as a pre-processing step, some points must be previously detected as anchors (i.e., those detected points are not deleted during the thinning process). The 2D order-independent algorithm proposed by Kardos et al. [6] is based on a strategy that partitions simple points into four classes in the first phase of an iteration. Thus, this solution lies far from the sequential thinning scheme according to Algorithm 1. Kardos and Palágyi also presented an alternative order-independent technique for pictures in arbitrary dimensions [5]. They used an endpoint characterization that had been also applied in some other 2D and 3D thinning algorithms. However, for the 3D case, this approach is only capable of producing medial surfaces.

In this paper, we introduce an isthmus-based solution for order-independency, which can be applied for 2D and 3D pictures and, unlike earlier order-independent al-

DOI: 10.2316/P.2012.778-025

gorithms, it makes also possible to generate centerlines for 3D objects.

The rest of this paper is organized as follows. Section 2 deals with the basic notions of digital topology. In Section 3 we propose our novel 2D and 3D sequential thinning algorithms, and we illustrate their results. The order-independency of the algorithms is proved in Section 4. Finally, we round off the paper with some concluding remarks.

2 Basic Notions and Results

We apply the basic concepts of digital topology as reviewed in [9].

Let p be a point in the nD digital space Z^n ($n \in \{2,3\}$). Then, we denote by $N_j(p)$ (for j = 4,8 in the 2D case and for j=6,18,26 in the 3D case) the set of points that are j-adjacent to point p and let $N_j^*(p) = N_j(p) \setminus \{p\}$ (see Fig. 1).

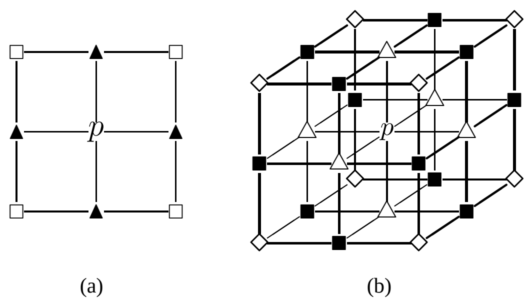

Figure 1. Frequently used adjacencies in $\mathbb{Z}^2$ (a). The set $N_4(p)$ contains the central point p and the 4 points marked "▲". The set $N_8(p)$ contains $N_4(p)$ and the 4 points marked "□".
Frequently used adjacency relations in $\mathbb{Z}^3$ (b). The set $N_6(p)$ contains p and the 6 points marked "△". The set $N_{18}(p)$ contains $N_6(p)$ and the 12 points marked "■". The set $N_{26}(p)$ contains $N_{18}(p)$ and the 8 points marked "◇"

The sequence of distinct points $\langle x_0, x_1, \ldots, x_n \rangle$ is called a j-path of length n from point x_0 to point x_n in a non-empty set of points X if each point of the sequence is in X and x_i is j-adjacent to x_{i-1} for each $1 \leq i \leq n$. Note that a single point is a j-path of length 0. Two points are said to be j- connected in the set X if there is a j-path in X between them (j = 4,8,6,18,26). A set of points X is j-connected in the set of points $Y \supseteq X$ if any two points in X are j-connected in Y (j = 4,8,6,18,26).

An nD $(k,\bar{k})$ binary digital picture $\mathcal{P} = (\mathbb{Z}^n, k, \bar{k}, B)$ is a quadruple [9], where $\mathbb{Z}^n$ is the set of nD discrete points ($n = 2$, $(k,\bar{k}) = (8,4)$ or $n = 3$, $(k,\bar{k}) = (26,6)$). Each point in $B \in \mathbb{Z}^n$ is called a black point and has a value of 1 assigned to it. Each point in $\mathbb{Z}^n \setminus B$ is called a white point and has a value of 0 assigned to it. An *object* is a maximal k-connected set of black points, while a *white component* is a maximal $\bar{k}$-connected set of white points.

A black point is called a *border point* in $(k,\bar{k})$ pictures if it is $\bar{k}$-adjacent to at least one white point.

The notion of simple points mentioned in Section 1 has various characterizations in 2D and 3D. Here we refer to the following ones:

Theorem 1 [9] *Black point p is simple in picture $(Z^2, 8, 4, B)$ if and only if all of the following conditions hold:*

1. *p is a border point.*
2. *The set $N_8^*(p) \cap B$ contains exactly one 8-component.*

Theorem 2 [10] *A black point p is simple in picture $(Z^3, 26, 6, B)$ if and only if all of the following conditions hold:*

1. *The set $N_{26}^*(p) \cap B$ contains exactly one 26-component.*
2. *The set $N_6(p) \setminus B$ is not empty.*
3. *Any two points in $N_6(p) \setminus B$ are 6-connected in the set $N_{18}(p) \setminus B$.*

Based on Theorems 1 and 2, the simplicity of a point p can be decided by examining the set $N_k(p)$ ($k = 8, 26$), hence it is a local property. Some configurations of simple and non-simple points in (8,4) and (26,6) pictures are shown in Figs. 2 and 3.

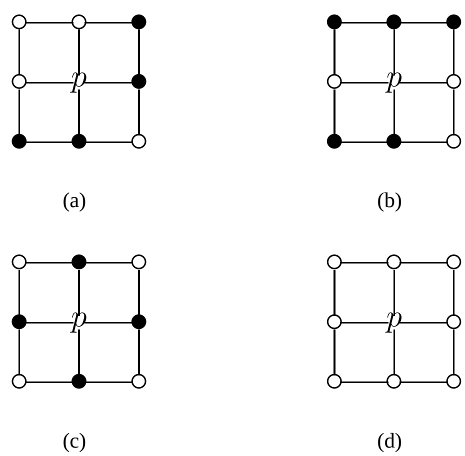

Figure 2. Examples for a simple (a) and three non-simple (b-d) points in (8,4) pictures. Point p is not simple in (b) since its deletion may split an object (Condition 2 of Theorem 1 is violated). A white 4-component (singleton cavity) is created by deletion of p in (c) (Condition 1 of Theorem 1 is violated). Point p is also not simple in (d), since its deletion completely deletes a (singleton) object (Condition 2 of Theorem 1 is violated)

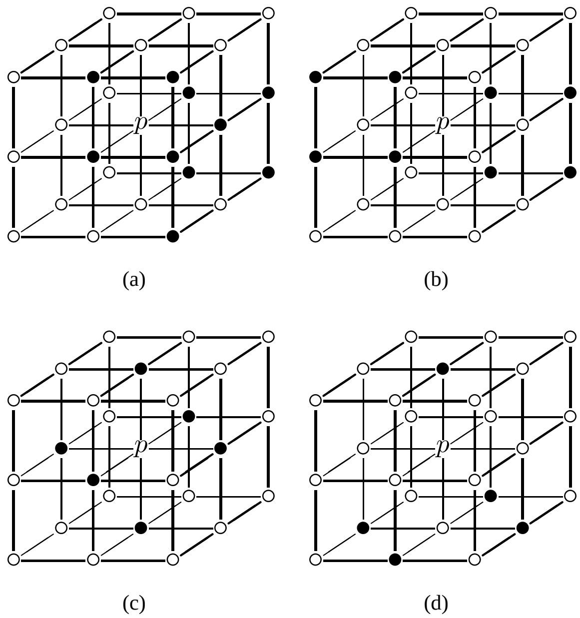

Figure 3. Examples for a simple (a) and three non-simple (b-d) points in (26,6) pictures. Point p is not simple in (b) since its deletion may split an object (Condition 1 of Theorem 2 is violated). A white 6-component (singleton cavity) is created by deletion of p in (c) (Condition 2 of Theorem 2 is violated). Point p is also not simple in (d), since its deletion may split an object and may create a hole (Conditions 2 and 3 of Theorem 2 are violated)

This paper presents three order-independent sequential thinning algorithms combined with isthmus-preservation. Our algorithms use the following characterizations of isthmuses.

Definition 1 *A border point p in a picture $(Z^2, 8, 4, B)$ is an $\mathcal{I}_C^2$-isthmus (for curve-thinning) if the set $N_8^*(p) \cap B$ contains more than one 8-component (i.e., Condition 2 of Theorem 1 is violated).*

Definition 2 *A border point p in a picture $(Z^3, 26, 6, B)$ is an $\mathcal{I}_C^3$-isthmus (for curve-thinning) if the set $N_{26}^*(p) \cap B$ contains more than one 26-component (i.e., Condition 1 of Theorem 2 is violated).*

Definition 3 *A border point p in a picture $(Z^3, 26, 6, B)$ is an $\mathcal{I}_S^3$-isthmus (for surface-thinning) if p is not a simple point (i.e., Condition 1 or Condition 3 of Theorem 2 is violated).*

Note that the latter characterizations in 3D correspond to the isthmuses proposed by Bertrand and Aktouf [1], with the exception that isolated (non-simple) points, which are not isthmuses by the terminology used in [1], are $\mathcal{I}_S^3$-isthmuses by Definition 3. Raynal and Couprie [13] used $\mathcal{I}_C^3$-isthmuses in their curve-thinning algorithm, however, they considered an alternative characterization for surface-isthmuses: a border point is an isthmus in their surface-thinning algorithm if Condition 3 of Theorem or 1 is violated. In order to produce medial surfaces that contain curves (i.e., 1D patches) for tubular parts, we consider that each $\mathcal{I}_C^3$-isthmus point is an $\mathcal{I}_S^3$-isthmus, too.

3 The Proposed Algorithms

Based on Definitions 1-3, we can write up our three isthmus-based sequential order-independent algorithms: one each for extracting 2D centerlines, 3D medial surfaces, and 3D centerlines. The scheme of these thinning algorithms denoted by KP-OIST-$\mathcal{I}$ ($\mathcal{I} \in \{\mathcal{I}_C^2, \mathcal{I}_C^3, \mathcal{I}_S^3\}$) are given by Algorithms 2-4.

In Phase 1 of Algorithms KP-OIST-$\mathcal{I}_C^2$ and KP-OIST-$\mathcal{I}_S^3$, simple points are collected in the set S, while detected isthmuses are accumulated in the constraint set I. In Phase 2, each collected point $p \in S$ is examined whether it would remain simple after the removal of some of the points being k-adjacent to p. Technically, the examination of this condition is carried out similarly, as it is described in [5]. If there exists a subset of simple neighbors, whose deletion would violate the simplicity of a given point $p \in S$, then the removal of p could result in order-dependency, otherwise it may be deleted. The algorithms stop if stability is reached.

Algorithm KP-OIST-$\mathcal{I}_C^3$ works similarly as the previous ones, with the exception that an additional examination is done in Phase 1, which needs particular explanation. Let us consider two flat 3D objects: an $m \times m \times 1$ and an $m \times m \times 2$ horizontal surface ($m > 2$, see Fig. 4 for such objects when $m = 7$). It is obvious that in the first object only the points on the edges are simple, but as the other points are not considered to be isthmuses, the algorithm removes the actual edge points in each iteration until it results in a small object contained by a $2 \times 2 \times 1$ region of Z^3. On the other hand, it is easy to see that the second object contains only simple points. Therefore, if we would put all of these points into S, no one of them could be deleted in Phase 2, as a given $p \in S$ would be an isolated point after the removal of all its black neighbors, which means that p would not satisfy the deleting condition in Phase 2. For this reason no one point in the second object could be removed, but this would lead to an incorrect result in the view of curve thinning. From Definition 3 follows that an object point p being in similar situation as mentioned before has a simple 6-neighbor q such that p would become an $\mathcal{I}_S^3$-isthmus after the removal of q. Thus, to avoid this problem, we construct an additional set Q for each simple point p in Phase 1, where we collect those critical 6-neighbors. Obviously, the case $Q = \emptyset$ implies that p must be on the edge of such special two-voxel wide objects, i.e., it can be removed.

Figs. 5-8 present some illustrative examples for 2D centerlines, 3D medial surfaces, and 3D centerlines produced by our new algorithms KP-OIST-$\mathcal{I}_C^2$, KP-OIST-$\mathcal{I}_S^3$, and KP-OIST-$\mathcal{I}_C^3$ compared with the corresponding algo-

(a)

(b)

Figure 4. The flat objects for the explanation of algorithm KP-OIST-$\mathcal{I}_\mathcal{C}^3$. (Their sizes are $7 \times 7 \times 1$ (a) and $7 \times 7 \times 2$ (b).)

rithms KP-OIST-2D and KP-OIST-3D described in [5]. Note that the medial surface and centerline of the capsule shown in Fig. 6 produced by algorithms KP-OIST-$\mathcal{I}_\mathcal{S}^3$ and KP-OIST-$\mathcal{I}_\mathcal{C}^3$ coincide, and this meets our expectation for such shape descriptors of tubular structures. However, one could easily check that if the definition of surface-isthmuses in [13] was used by the algorithm KP-OIST-$\mathcal{I}_\mathcal{S}^3$, it would generate a single isolated object point as the medial surface of the capsule. This confirms the correctness of our definition of surface-isthmuses (see Definition 3) in contrast to the one in [13].

Algorithm 2: KP-OIST-$\mathcal{I}_\mathcal{C}^2$

Input: picture $(Z^2, 8, 4, X)$
Output: picture $(Z^2, 8, 4, Y)$
$Y = X$
$I = \emptyset$
repeat
  // *Phase 1: contour tracking*
  $S = \emptyset$
  foreach $p \in Y \setminus I$ **do**
    if p is a simple point in Y **then**
      $S = S \cup \{p\}$
    else if p is an $\mathcal{I}_\mathcal{C}^2$-isthmus in Y **then**
      $I = I \cup \{p\}$
  // *Phase 2: reduction*
  changed = false
  foreach $p \in S$ **do**
    deletable = true
    D = { $q \mid q \in N_8^*(p) \cap Y \cap S$ }
    foreach $\Delta \subseteq D$ **do**
      if p is not simple in $(Z^2, 8, 4, Y \setminus \Delta)$ **then**
        deletable = false
        break
    if deletable = true **then**
      $Y = Y \setminus \{p\}$
      changed = true
until changed = false;

4 Verification

It is straightforward that algorithms KP-OIST-$\mathcal{I}_\mathcal{C}^2$, KP-OIST-$\mathcal{I}_\mathcal{S}^3$, and KP-OIST-$\mathcal{I}_\mathcal{C}^3$ remove only simple points, and as sequential algorithms remove only one point at a time, we can state that the above algorithms preserve topology. Here we prove, that they are also order-independent.

Theorem 3 *Algorithms KP-OIST-$\mathcal{I}$ ($\mathcal{I} \in \{\mathcal{I}_\mathcal{C}^2, \mathcal{I}_\mathcal{S}^3, \mathcal{I}_\mathcal{C}^3\}$) are order-independent.*

Proof. It is sufficient to see that order-independency holds for an iteration step of the algorithms. In Phase 1, no points are removed, and the content of sets S and Q does not depend on the visiting order of object points.

Let us suppose that in Phase 2, an arbitrary simple point $p \in S$ is visited before its k-neighbors, and it will be deleted. By Theorems 1 and 2, the simplicity of a point p depends only on the set $N_k(p)$ ($k \in \{8, 26\}$, accordingly to the type of algorithm), hence if $N_k^*(p) \cap S = \emptyset$, then p will be necessarily removed. Let us examine the case when $N_k^*(p) \cap S \neq \emptyset$, and let $\Delta \subseteq D$. As p is visited before any $q \in \Delta$, by the deleting condition p is also simple in $Y \setminus \Delta$. $(D \setminus \Delta) \subseteq D$ implies that for any $\Delta' \subseteq D \setminus \Delta$, $\Delta' \subseteq D$ holds, as well, hence p also satisfies the deleting condition in $Y \setminus \Delta$.

Now, let us assume that $p \in S$ will not be deleted, when it is visited before its k-neighbors. Then, there must be a set $\Delta \subseteq D$ such that p is not simple in $Y \setminus \Delta$. We show indirectly that in this case Δ may not be deleted. Thus, we suppose that the algorithms remove all points of Δ. This means that any $q \in \Delta$ must fulfill the deleting condition in the beginning of Phase 2, and as $p \in N_k(q)$, it is not hard to see that q is simple in $Y \setminus ((\Delta \cup \{p\}) \setminus \{q\})$. From this follows that the removal of the set $\Delta \cup \{p\}$ preserves topology. However, this means a contradiction with the fact that p is not simple in $Y \setminus \Delta$.

Therefore, p is removed by algorithms KP-OIST-$\mathcal{I}$ if and only if it fulfills their deleting condition in the beginning of Phase 2, which implies that algorithms KP-OIST-$\mathcal{I}$ are order-independent. □

5 Conclusion

This paper introduces three new order-independent sequential thinning algorithms working on 2D and 3D binary pictures. The algorithms are based on isthmuses (instead of the conventional endpoint-preservation thinning scheme). Our test results show that the proposed algorithms produce less unwanted skeletal branches then the conventional endpoint-based ones. As another major contribution, this work presents the first 3D order-independent sequential

Algorithm 3: KP-OIST-$\mathcal{I}_\mathcal{S}^3$

Input: picture $(Z^3, 26, 6, X)$
Output: picture $(Z^3, 26, 6, Y)$
$Y = X$
$I = \emptyset$
repeat
    // *Phase 1: contour tracking*
    $S = \emptyset$
    foreach $p \in Y \setminus I$ **do**
        if p is a simple point in Y **then**
            $S = S \cup \{p\}$
        else if p is an $\mathcal{I}_\mathcal{S}^3$-isthmus in Y **then**
            $I = I \cup \{p\}$
    // *Phase 2: reduction*
    changed = false
    foreach $p \in S$ **do**
        deletable = true
        D = { $q \mid q \in N_{26}^*(p) \cap Y \cap S$ }
        foreach $\Delta \subseteq D$ **do**
            if p is not simple in $(Z^3, 26, 6, Y \setminus \Delta)$ **then**
                deletable = false
                break
        if deletable = true **then**
            $Y = Y \setminus \{p\}$
            changed = true
until changed = false;

Algorithm 4: KP-OIST-$\mathcal{I}_\mathcal{C}^3$

Input: picture $(Z^3, 26, 6, X)$
Output: picture $(Z^3, 26, 6, Y)$
$Y = X$
$I = \emptyset$
repeat
    // *Phase 1: contour tracking*
    $S = \emptyset$
    foreach $p \in Y \setminus I$ **do**
        Q = { $q \mid q \in N_6^*(p) \cap Y$, q is simple, and p is an $\mathcal{I}_\mathcal{S}^3$-isthmus in $Y \setminus \{q\}$}
        if p is a simple point in Y **and** $Q = \emptyset$ **then**
            $S = S \cup \{p\}$
        else if p is an $\mathcal{I}_\mathcal{C}^3$-isthmus in Y **then**
            $I = I \cup \{p\}$
    // *Phase 2: reduction*
    changed = false
    foreach $p \in S$ **do**
        deletable = true
        D = { $q \mid q \in N_{26}^*(p) \cap Y \cap S$ }
        foreach $\Delta \subseteq D$ **do**
            if p is not simple in $(Z^3, 26, 6, Y \setminus \Delta)$ **then**
                deletable = false
                break
        if deletable = true **then**
            $Y = Y \setminus \{p\}$
            changed = true
until changed = false;

thinning algorithm for producing centerlines.

Acknowledgements

This research was supported by the European Union and the European Regional Development Fund under the grant agreements TÁMOP-4.2.1/B-09/1/KONV-2010-0005 and TÁMOP-4.2.2/B-10/1-201-0012, and the grant CNK80370 of the National Office for Research and Technology (NKTH) & the Hungarian Scientific Research Fund (OTKA).

References

[1] G. Bertrand, Z. Aktouf, A 3D thinning algorithm using subfields, *SPIE Proc. of Conf. on Vision Geometry*, San Diego, CA, USA, 1994, 113–124

[2] G. Bertrand, M. Couprie, Transformations topologiques discrètes, in Coeurjolly, D., Montanvert, A., Chassery J. (Eds.), *Géométrie discrète et images numériques*, Hermès, 2007, 187–209

[3] R.W. Hall, Parallel connectivity–preserving thinning algorithm, in Kong, T.Y., Rosenfeld, A. (Eds.), *Topological Algorithms for Digital Image Processing, Machine Intelligence and Pattern Recognition*, 19, (Amsterdam, Elsevier Science, 1996) 145–179

[4] M. Iwanowski, P. Soille, Order independence in binary 2D homotopic thinning, *Proc. 13th International Conference on Discrete Geometry for Computer Imagery, DGCI 2006, Lecture Notes in Computer Science 4245*, 2006, 592–604

[5] P. Kardos, K. Palágyi, Order-independent sequential thinning in arbitrary dimensions, *Proc. IASTED International Conference on Signal and Image Processing and Applications, SIPA 2011*, 2011, 129–134

[6] P. Kardos, G. Németh, K. Palágyi, An order–independent sequential thinning algorithm, *Proc. 13th International Workshop on Combinatorial Image Analysis, IWCIA 2009, Lecture Notes in Computer Science 5852*, 2009, 162–175

[7] T.Y. Kong, On topology preservation in 2-d and 3-d thinning, *International Journal of Pattern Recognition and Artificial Intelligence*, 9, 1995, 813–844

[8] T.Y. Kong, Topology-preserving deletion of 1's from 2-, 3- and 4-dimensional binary images, *Proc. 7th Int.*

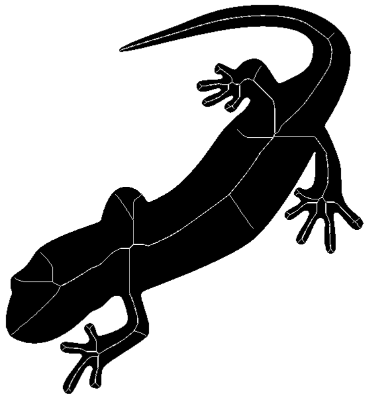

(a) KP-OIST-2D (3 072)

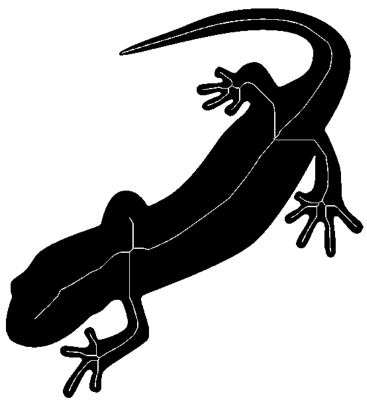

(b) KP-OIST-$\mathcal{I}_{\mathcal{C}}^2$ (2 894)

Figure 5. A 552×607 image with $108\,615$ object points of a salamander and the results superimposed on the original object. The centerlines were produced by algorithm KP-OIST-2D presented in [5] (a) and by our new algorithm KP-OIST-$\mathcal{I}_{\mathcal{C}}^2$ (b). Numbers in parentheses indicate the count of object pixels

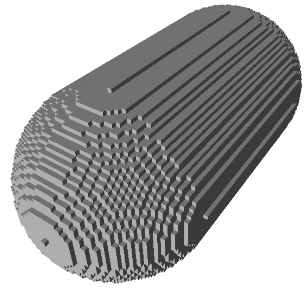

(a) original image (131 880)

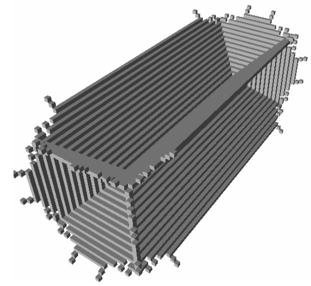

(b) KP-OIST-3D (4 946)

(c) KP-OIST-$\mathcal{I}_{\mathcal{S}}^3$, KP-OIST-$\mathcal{I}_{\mathcal{C}}^3$ (48)

Figure 6. A $100 \times 50 \times 50$ image of a capsule (a), its medial surface produced by algorithm KP-OIST-3D presented in [5] (b) and the same results of our new algorithms KP-OIST-$\mathcal{I}_{\mathcal{S}}^3$ and KP-OIST-$\mathcal{I}_{\mathcal{C}}^3$ (c). Note that KP-OIST-$\mathcal{I}_{\mathcal{S}}^3$ can produce curves for tubular structures. Numbers in parentheses indicate the count of object pixels

Workshop Discrete Geometry for Computer Imagery, Lecture Notes in Computer Science 1347, 1997, 3–18

[9] T.Y. Kong, A. Rosenfeld, Digital topology: Introduction and survey, *Computer Vision, Graphics, and Image Processing*, 48, 1989, 357–393

[10] G. Malandain, G. Bertrand, Fast characterization of 3D simple points, *Proc. 11th IEEE Internat. Conf. on Pattern Recognition, ICPR'92*, 1992, 232–235

[11] L. Lam, S.-W. Lee, C.Y. Suen, Thinning methodologies – A comprehensive survey, *IEEE Trans. Pattern Analysis and Machine Intelligence*, 14, 1992, 869–885

[12] V. Ranwez, P. Soille, Order independent homotopic thinning for binary and grey tone anchored skeletons, *Pattern Recognition Letters*, 23(6), 2002, 687–702

[13] B. Raynal, M. Couprie, Isthmus-based 6-directional parallel thinning algorithms, *Proc. 16th IAPR International Conference on Discrete Geometry for Computer Imagery, DGCI 2011*, *Lecture Notes in Computer Science 6607*, 2011, 175–186

[14] A. Rosenfeld, Connectivity in digital pictures, *Journal of the Association for Computer Machinery*, 17, 1970, 146–160

[15] K. Siddiqi, S. Pizer, *Medial Representations: Mathematics, Algorithms and Applications* (New York, Springer, 2008)

[16] C.Y. Suen, P.S.P. Wang, *Thinning Methodologies for Pattern Recognition, Series in Machine Perception and Artificial Intelligence 8* (Singapore, World Scientific, 1994)

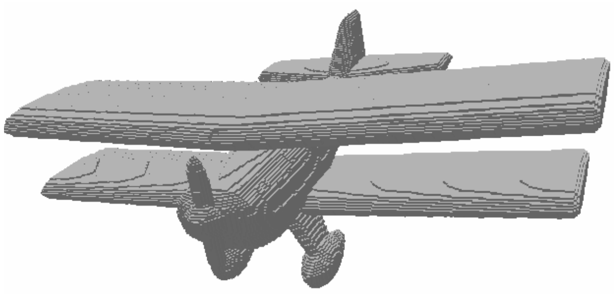

(a) original image (656 424)

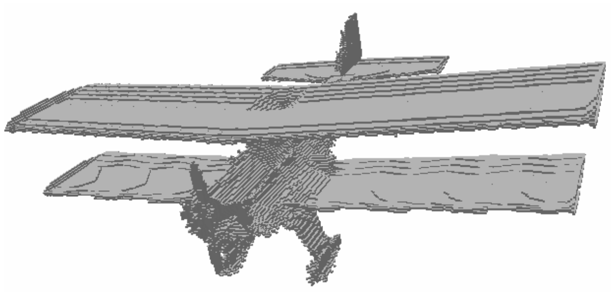

(b) KP-OIST-3D (74 565)

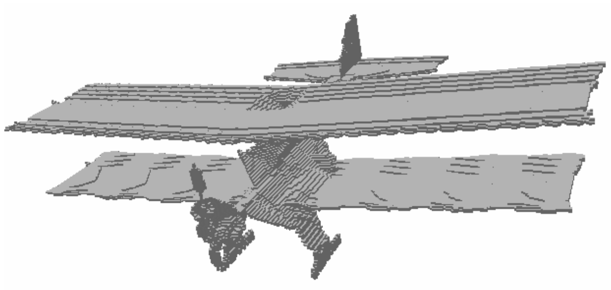

(c) KP-OIST-$\mathcal{I}_{\mathcal{S}}^3$ (74 122)

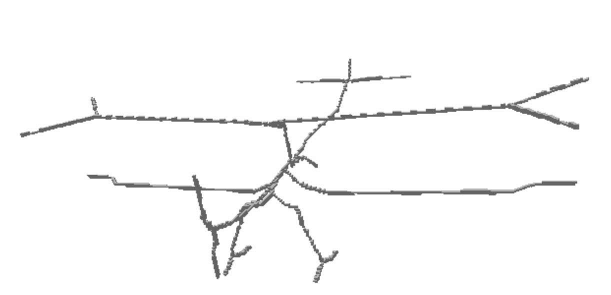

(d) KP-OIST-$\mathcal{I}_{\mathcal{C}}^3$ (2 320)

Figure 7. A $217 \times 304 \times 98$ image of a plane (a), its medial surfaces produced by algorithm KP-OIST-3D presented in [5] (b) and by our new algorithm KP-OIST-$\mathcal{I}_{\mathcal{S}}^3$, and centerline resulted by our new algorithm KP-OIST-$\mathcal{I}_{\mathcal{C}}^3$ (d). Numbers in parentheses indicate the count of object pixels

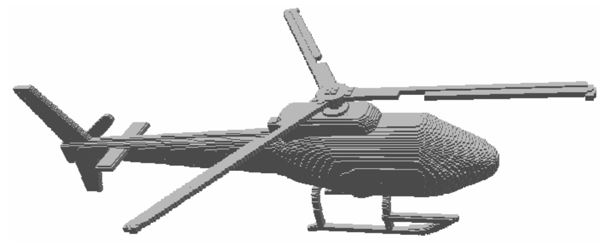

(a) original image (273 743)

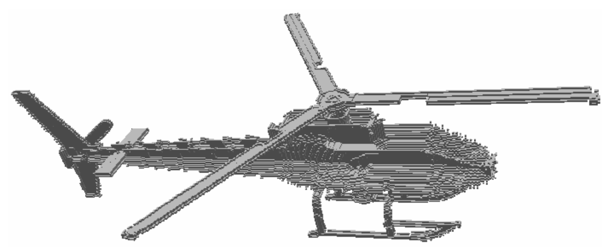

(b) KP-OIST-3D (28 211)

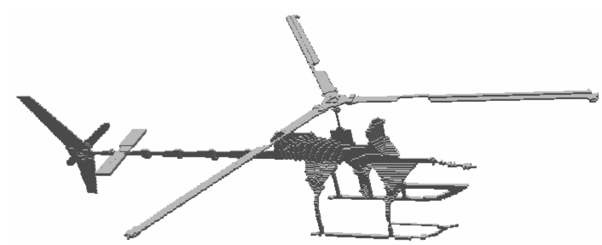

(c) KP-OIST-$\mathcal{I}_{\mathcal{S}}^3$ (12 512)

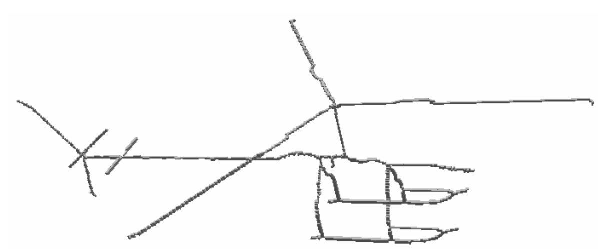

(d) KP-OIST-$\mathcal{I}_{\mathcal{C}}^3$ (2 810)

Figure 8. A $102 \times 381 \times 255$ image of a helicopter (a), its medial surfaces produced by algorithm KP-OIST-3D presented in [5] (b) and by our new algorithm KP-OIST-$\mathcal{I}_{\mathcal{S}}^3$, and centerline resulted by our new algorithm KP-OIST-$\mathcal{I}_{\mathcal{C}}^3$ (d). Numbers in parentheses indicate the count of object pixels